Stem Cell Research 16 (2016) 776–781

Contents lists available at ScienceDirect

Stem Cell Research

journal homepage: www.elsevier.com/locate/scr

Short Report

Comparative transcriptome analysis in induced neural stem cells reveals defined neural cell identities *in vitro* and after transplantation into the adult rodent brain

Anna-Lena Hallmann [a,b,1], Marcos J. Araúzo-Bravo [c,d,1], Christina Zerfass [a], Volker Senner [a], Marc Ehrlich [a,b], Olympia E. Psathaki [b], Dong Wook Han [e], Natalia Tapia [b,f], Holm Zaehres [b], Hans R. Schöler [b], Tanja Kuhlmann [a,2], Gunnar Hargus [a,b,g,*,2]

[a] *Institute of Neuropathology, University Hospital Münster, 48149 Münster, Germany*
[b] *Max Planck Institute for Molecular Biomedicine, 48149 Münster, Germany*
[c] *Group of Computational Biology and Systems Biomedicine, Biodonostia Health Research Institute, 20014 San Sebastián, Spain*
[d] *IKERBASQUE, Basque Foundation for Science, 48011 Bilbao, Spain*
[e] *Department of Stem Cell Biology, School of Medicine, Konkuk University, 143701 Seoul, Republic of Korea*
[f] *Institute of Biomedicine of Valencia, Spanish National Research Council (IBV-CSIC), Jaime Roig 11, 46010 Valencia, Spain*
[g] *Department of Pathology and Cell Biology, Columbia University Medical Center, 10032 New York, USA*

ARTICLE INFO

Article history:
Received 21 November 2015
Received in revised form 21 February 2016
Accepted 15 April 2016
Available online 19 April 2016

Keywords:
Induced neural stem cells
Neural stem cells
Transplantation
Transcriptome
Regional programs

ABSTRACT

Reprogramming technology enables the production of neural progenitor cells (NPCs) from somatic cells by direct transdifferentiation. However, little is known on how neural programs in these induced neural stem cells (iNSCs) differ from those of alternative stem cell populations *in vitro* and *in vivo*. Here, we performed transcriptome analyses on murine iNSCs in comparison to brain-derived neural stem cells (NSCs) and pluripotent stem cell-derived NPCs, which revealed distinct global, neural, metabolic and cell cycle-associated marks in these populations. iNSCs carried a hindbrain/posterior cell identity, which could be shifted towards caudal, partially to rostral but not towards ventral fates *in vitro*. iNSCs survived after transplantation into the rodent brain and exhibited *in vivo*-characteristics, neural and metabolic programs similar to transplanted NSCs. However, iNSCs vastly retained caudal identities demonstrating cell-autonomy of regional programs *in vivo*. These data could have significant implications for a variety of *in vitro*- and *in vivo*-applications using iNSCs.

1. Introduction

Over the past few years, significant progress has been made to derive expandable neural progenitor cell (NPC) populations for biomedical research and regenerative medicine. One important cell source comprises pluripotent stem cells such as embryonic stem cells (ESCs) or induced pluripotent stem cells (iPSCs), which can be efficiently differentiated into expandable NPCs and subsequently into mature neurons and glial cells using established differentiation protocols. In fact, several groups have demonstrated successful application of ESC- or iPSC–NPC-derived neural cells in disease modeling assays or for cell replacement in animal models of neurological disorders (Ehrlich et al., 2015; Hargus et al., 2010; Hargus et al., 2014b; Kriks et al., 2011; Reinhardt et al., 2013; Ross and Akimov, 2014).

Further refinements of reprogramming technologies allowed for the derivation of NPCs by direct conversion of fibroblasts into induced neural stem cells (iNSCs) using different combinations of classical reprogramming and neural transcription factors (Cassady et al., 2014; Han et al., 2012; Kim et al., 2011; Kim et al., 2014; Lujan et al., 2012; Ring et al., 2012; Sheng et al., 2012; Thier et al., 2012). These iNSCs carry self-renewing capabilities and were found to resemble neural stem cells (NSCs) from the developing brain. Like NSCs, iNSCs readily differentiate into neuronal and glial derivatives *in vitro* when appropriate differentiation cues are provided. Similar to the process of iPSC derivation, iNSC generation is a gradual process, which involves silencing of transgenes and of donor cell-type specific transcriptional programs as well as step-wise establishment of stem cell identities during initial

Abbreviations: iNSCs, Induced neural stem cells; NSCs, Neural stem cells; ESCs, Embryonic stem cells; NPCs, Neural progenitor cells; iPSCs, Induced pluripotent stem cells; GFP, Green fluorescent protein; FACS, Fluorescent-activated cell sorting; DEGs, Differentially expressed genes; GO, Gene ontology; ER, Endoplasmic reticulum; RA, Retinoic acid; Dcx, Doublecortin; SVZ, Subventricular zone.

* Corresponding author at: Institute of Neuropathology, University Hospital Münster, Pottkamp 2, 48149 Münster, and Max Planck Institute for Molecular Biomedicine, Röntgenstrasse 20, 48149 Münster, Germany.
E-mail address: gunnar.hargus@ukmuenster.de (G. Hargus).
[1] Co-first author.
[2] Co-senior author.

http://dx.doi.org/10.1016/j.scr.2016.04.015

propagation of cells (Han et al., 2012). iNSC direct reprogramming technology reduces the potential risk of tumor formation, which may occur when using ESC- or iPSC-derived neural cell populations for cell transplantation. As such, successful engraftment but no tumor formation was seen after transplantation of iNSCs into the brain and spinal cord of adult mice (Han et al., 2012; Hemmer et al., 2014; Hong et al., 2014; Liu et al., 2015).

Despite these achievements in iNSC technology, little is known on how cellular identities of iNSCs differ from those of NSCs in comparison to pluripotent stem cell-derived NPCs. For instance, it is currently unknown to what extent neural, metabolic and stress response pathways differ between these neural cell populations, although ESC–NPCs have previously been included as a neural cell population in a comparative study on iNSCs (Cassady et al., 2014). It is also not known if positional neural cell identities in iNSCs are irreversibly established or if they can be shifted along the rostro-caudal or ventro-dorsal axis as demonstrated for ESC-derived NPCs (Bertacchi et al., 2013). Furthermore, data are lacking on whether neural positional marks in iNSCs remain stable or change after transplantation into the adult rodent brain. These data could have significant implications for biomedical applications using iNSCs such as disease modeling or cell replacement therapy since cells with appropriate neural programs may have to be derived for these purposes. To address these questions, we have derived iNSCs from fibroblasts by transcription factor-mediated transdifferentiation and performed comparative studies on iNSCs both *in vitro* and *in vivo*.

2. Materials and methods

Please see the Supplemental Information for further details. Data of at least three independent experiments are presented as mean + SEM. Statistical significance was determined by unpaired Student's t-test.

3. Results

3.1. iNSCs carry specific neural cell identities in vitro

We derived iNSCs from murine fibroblasts by transduction with retroviruses expressing *Pou3f4* (also known as *Brn4*), *Klf4*, *c-Myc* and *Sox2*. This combination of reprogramming factors efficiently generates iNSCs within 5 weeks of initial transduction as previously described (Han et al., 2012; Kim et al., 2014). iNSCs were morphologically indistinguishable from primary murine NSCs, which had been isolated from mouse embryonic forebrains (Fig. 1A). Immunocytochemical analyses of iNSCs and NSCs revealed comparably strong expression of the neural signature genes *Nestin* and *Olig2* (Fig. 1A). This finding was confirmed by qPCR showing strong expression of *Nestin*, *Olig2*, *Pax6* and *Sox2* in both iNSCs and NSCs (Fig. S1A). Both NSCs and iNSCs showed robust differentiation into βIII-tubulin$^+$ neurons (NSCs: 29.9 ± 1.6%; iNSCs: 28.6 ± 3.0%) and GFAP$^+$ astrocytes (NSCs: 69.3 ± 2.1%; iNSCs: 71.0 ± 2.4%; Fig. S1B–D) demonstrating successful derivation of iNSCs.

We next characterized transcriptome profiles in iNSCs in comparison to NSCs and pluripotent stem cell-derived NPCs, all of which comprise neural progenitor populations with propagation and neural cell differentiation capabilities (Fig. 1B). We applied bioinformatics analyses on our transcriptome data to perform clustering analysis, to search for differentially expressed genes (DEGs), to perform gene ontology (GO) statistical enrichment analysis and to obtain expression patterns of genes involved in neural development and cellular metabolism (Fig. 1C–E and Fig. S1E–K). NPCs were differentiated from murine ESCs, which appeared morphologically indistinguishable from NSCs and iNSCs (Fig. 1B). We collected whole genome expression profiles from iNSCs, NSCs and ESC–NPCs and included mouse embryonic fibroblasts as the starting population of iNSCs (Fig. 1C–D). Hierarchical clustering analysis revealed that all neural cell populations including iNSCs clearly separated as a group from mesoderm-derived fibroblasts confirming efficient neural conversion of iNSCs. At the same time, iNSCs, NSCs and ESC–NPCs formed distinct independent cell groups, which clearly separated from each other. Notably, iNSCs clustered closest to NSCs and, together with NSCs, separated from ESC–NPCs indicating that overall expression programs in iNSCs were more similar to those in NSCs than in ESC-derived NPCs.

We next examined DEGs and their functional annotations in iNSCs, NSCs and ESC–NPCs (Table S1). We found 465 upregulated genes and 754 downregulated genes in iNSCs compared to ESC–NPCs and a much lower number of genes, 111 upregulated genes and 233 downregulated genes, in iNSCs compared to NSCs. Upregulated genes in iNSCs compared to ESC–NPCs were significantly enriched for GO terms such as *nervous system development*, *neurological system process*, *signal transduction* and *amino acid and derivative metabolic process*, while downregulated genes were related to *cell cycle-associated processes*, *cell migration* and *anatomical structure and brain development*. On the other hand, upregulated genes in iNSCs in comparison to NSCs were associated with GO terms such *organ morphogenesis*, *organ and cell development* and *regulation of apoptosis*, while downregulated genes were related to *central nervous system and brain development*, *cell-cell signaling* and *amino acid and derivative metabolic process* (see Table S1 for complete list of genes). These findings suggested that iNSCs comprise a defined neural cell population with characteristic developmental marks and metabolic and cell regulatory programs.

To further characterize these neural programs in iNSCs, we performed a directed comparative analysis of neural, metabolism-, stress- and cell cycle-associated genes in all three neural cell populations. An analysis of 109 brain-associated neural genes revealed close clustering of iNSCs and NSCs and clear separation of ESC–NPCs from iNSCs and NSCs as seen in the whole genome expression analysis (Fig. 1E, Fig. S1E). Interestingly, iNSCs demonstrated especially strong expression of the neural genes *Olig1*, *Olig2*, *Ctnnd2*, *Aqp4*, *Mt3*, *Cspg5*, *Cmtm5*, *Plp1* and *Gfap*, while *Nxph1*, *Dcx and Dpp10*, genes with forebrain- and cortical development-associated functions, were expressed at much lower levels in iNSCs (Fig. S1E). We furthermore found a similar hierarchical cluster profile when comparing the expression of 31 oxidative stress-associated genes (Fig. S1F, Fig. S2A), 50 heat shock protein-coding genes (Fig. S1G, Fig. S2C), 68 endoplasmic reticulum (ER) stress-associated genes (Fig. S1H, Fig. S2B) and of 65 ubiquitination-associated genes (Fig. S1I, Fig. S2D). Interestingly and in line with our previous observation as described above, iNSCs as well as NSCs also separated from ESC–NPCs when examining the expression profile of 71 cell-cycle-associated genes (Fig. S1J–K). Taken together, these findings indicated distinct differences in the control of neural, cell cycle, metabolic and stress response pathways in these neural cell populations with a higher similarity between iNSCs and NSCs than between iNSCs and ESC–NPCs and between NSCs and ESC–NPCs.

3.2. The positional identity of iNSCs is differentially influenced by patterning factors in vitro

We next set out to define the regional identity of iNSCs along the rostro-caudal axis in comparison to NSCs and ESC–NPCs. To this end, we examined the expression of *Foxg1*, *Lhx2*, *Emx2*, *Dlx1*, *Dlx2*, *Otx2*, *En1*, *En2*, *Foxa2*, *Hoxa2*, *Hoxd3*, *Hoxb4*, *Hoxd4*, *Hoxa5* and *Hoxc6* in iNSCs, NSCs and ESC–NPCs (Fig. 1F, Fig. S1L–M). As expected, forebrain-derived NSCs expressed high levels of the rostral markers *Foxg1*, *Dlx1*, *Dlx2* and *Otx2* (Fig. 1F, Fig. S1L). In contrast, iNSCs expressed high levels of the caudal markers *Hoxa2*, *Hoxb4*, *Hoxd4*, *Hoxa5* and *Hoxc6*, while rostral markers were almost not expressed establishing a hindbrain/posterior cell identity rather than a forebrain identity in iNSCs (Fig. 1F, Fig. S1M). These findings are in line with our observation of decreased expression of cortex-associated genes *in vitro* (Fig. S1E). Interestingly, ESC–NPCs expressed high levels of the rostral markers *Foxg1*

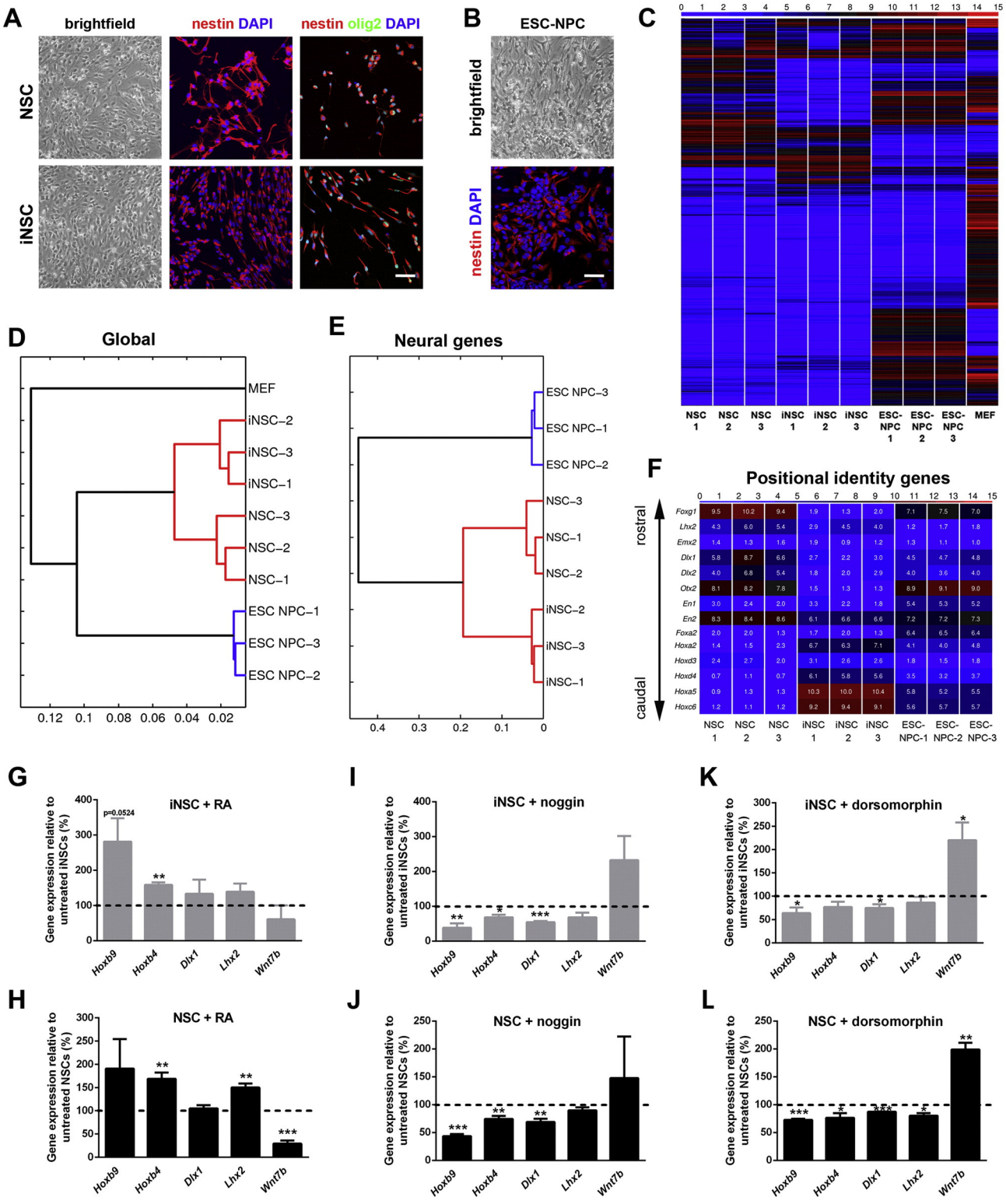

Fig. 1. iNSCs carry specific global, neural and regional cell identities *in vitro* (A) Brightfield images and immunostainings of NSCs and iNSCs for Nestin (red) and Olig2 (green). Nuclei were counterstained with DAPI (blue). Scale bar = 50 μm. (B) Brightfield image of ESC–NPCs and immunostaining of ESC–NPCs for Nestin (red). Nuclei were counterstained with DAPI (blue). Scale bar = 50 μm. (C–D) Heatmap (C) and hierarchical cluster dendrogram (D) demonstrating whole genome expression profiles of NSCs (NSC-1,-2,-3), iNSCs (iNSC-1,-2,-3), ESC-derived NPCs (ESC–NPC-1,-2,-3) and fibroblasts (MEF). Samples represent biological replicates. (E) Hierarchical cluster dendrogram of 109 brain-associated neural genes. (F) Heatmap of regional marker gene expression along the rostro-caudal axis in NSCs (NSC-1,-2,-3) and iNSCs (iNSC-1,-2,-3). Note the strong expression of rostral genes in NSCs and the strong expression of caudal genes in iNSCs. (G–L) qRT–PCR expression profiles of regional identity genes in iNSCs (G, I, K) and NSCs (H, J, L) after administration of RA (G–H), noggin (I–J) or dorsomorphin (K–L). Data are presented as mean of replicates from three independent patterning experiments + SEM. Unpaired t-test was used as statistical test (*p: <0.05; **p: <0.005; ***p: <0.001).

and *Otx2* but also increased levels of the caudal markers *Hoxa5* and *Hoxc6*, pointing towards a less defined regional identity of ESC–NPCs along the rostro-caudal axis (Fig. 1F).

We next tested if positional marks in iNSCs could be modified by culturing cells in the presence of the caudalising factor retinoic acid (RA) or in the presence of the rostralising factors noggin and dorsomorphin. We

applied incubation time frames and factor concentrations, which have previously been reported to efficiently direct ESCs towards caudal and rostral fates during neural differentiation (Fig. 1G–L; Bertacchi et al., 2013).

Application of RA for 4 days in iNSCs resulted in significantly elevated levels of *Hoxb4* and a tendency towards increased expression of *Hoxb9* (p-value = 0.0524) indicating that increased expression of caudal positional marks in iNSCs could be achieved *in vitro* (Fig. 1G). Similar results were obtained for NSCs, which were cultured in parallel (Fig. 1H). In contrast to these caudalising experiments, application of noggin to iNSCs for 4 days did not result in significantly increased expression of rostral forebrain markers but caused significantly reduced expression of *Hoxb4* and *Hoxb9* (Fig. 1I). Rostralising effects in iNSCs were more pronounced after administration of dorsomorphin for 4 days, which also caused decreased expression of caudal markers but additionally resulted in significantly elevated levels of the rostral marker *Wnt7b* (Fig. 1K). However, neither noggin nor dorsomorphin was able to induce the expression of *Foxg1* in iNSCs, which was only unreliably detected in cultures after treatment and is thus not shown here. Thus, iNSCs could only partially be directed towards rostral fates *in vitro*. Again, similar responses were seen in NSCs, which received noggin and dorsomorphin in parallel (Fig. 1J and L). We finally tested if regional programs in iNSCs and NSCs could be shifted along the ventro-dorsal axis by administration of sonic hedgehog to generate floor plate cells expressing the ventral marker genes *En1* and *Foxa2*, which, however, could not be achieved in either group. Thus, our findings indicated that regional identities in iNSCs could be shifted towards caudal, partially to rostral but not towards ventral fates *in vitro*.

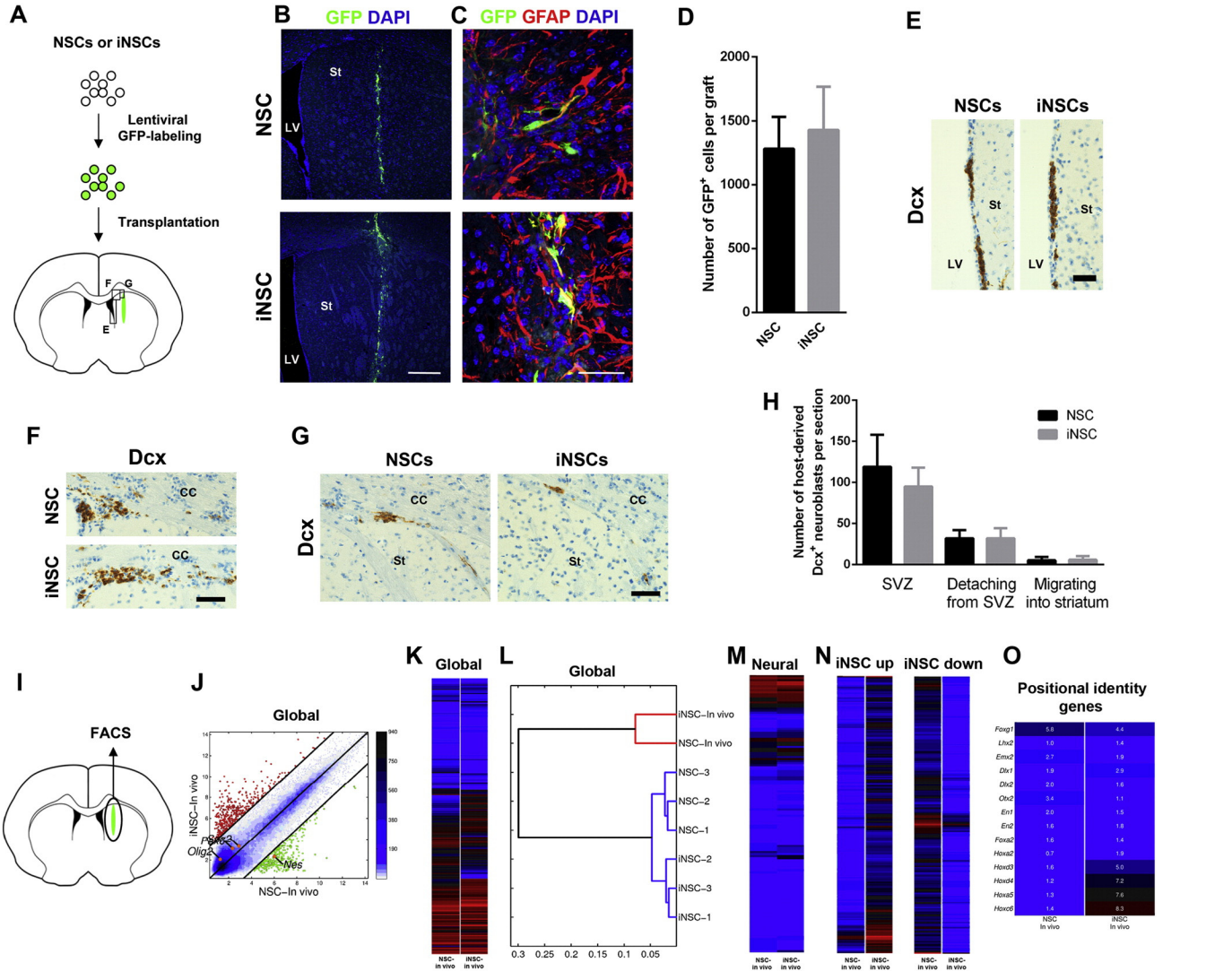

Fig. 2. iNSCs survive after transplantation into the adult rodent brain and retain their positional neural cell identity *in vivo*. (A) Schematic drawing demonstrating GFP labeling and transplantation of NSCs and iNSCs into the striatum of adult mice. Boxes indicate areas for quantification of doublecortin$^+$ (Dcx$^+$) neuroblasts. (B–C) Immunohistochemical images of transplanted NSCs and iNSCs expressing GFP (B–C) and GFAP (C). Nuclei were counterstained with DAPI. LV = Lateral ventricle; St = Striatum. Scale bar in B = 200 μm. Scale bar in C = 50 μm. (D) Quantification of GFP$^+$ NSCs and iNSCs within grafts 14 days after transplantation. Data are presented as mean of six independent biological replicates + SEM (n = 6 grafts per group). (E–G) Immunostainings of host-derived Dcx$^+$ neuroblasts in the subventricular zone (SVZ, E), of neuroblasts detaching from the SVZ (F) and of neuroblasts migrating into the striatum (G). Nuclei were counterstained with hematoxylin. Scale bars in E, F and G = 50 μm. (H) Quantification of host-derived Dcx$^+$ neuroblasts after transplantation of NSCs and iNSCs as depicted in E–G. Data are presented as mean of six independent biological replicates + SEM. (I–O) Transplanted NSCs and iNSCs were isolated from the mouse brain *via* FACS (I) to determine gene expression profiles. (J) Pairwise scatterplot comparing transcriptome profiles between transplanted NSCs (NSC–*In vivo*) and transplanted iNSCs (iNSC–*In vivo*). (K–L) Heatmap (K) and hierarchical cluster diagram (L) showing whole genome expression profiles in transplanted NSCs and iNSCs. (M) Heatmap of neural genes expressed in transplanted NSCs and iNSCs. (N) Heatmaps depicting differentially up- and downregulated genes in transplanted iNSCs compared to transplanted NSCs. (O) Heatmap of positional identity genes expressed in transplanted NSCs and iNSCs.

3.3. iNSCs survive after transplantation into the adult rodent brain and retain their positional neural cell identity in vivo

We next transplanted iNSCs and NSCs into the adult rodent forebrain to determine cell survival, graft–host interaction and neural and regional programs of transplanted cells *in vivo* (Fig. 2). In fact, this approach allowed us to determine if positional identities remained stable in engrafted iNSCs or if they were influenced by a forebrain microenvironment leading to a more complete rostralisation of cells *in vivo*. We transduced iNSCs and NSCs with a lentivirus expressing green fluorescent protein (GFP) before transplantation resulting in GFP positivity in more than 95% of cells in both groups. GFP-labeled iNSCs or NSCs were transplanted into the striatum of adult C57BL6J mice and grafts were analyzed 14 days after transplantation (Fig. 2A–D). This analysis revealed equal numbers of surviving NSCs (1282 ± 248) and iNSCs (1428 ± 339) in the striatum, the site targeted for transplantation (Fig. 2B–D). Engrafted NSCs and iNSCs presented with abundant cellular projections and mainly expressed GFAP (Fig. 2C). Since previous studies have demonstrated that transplanted neural cells have the capability to attract migrating, doublecortin $(Dcx)^+$ neuroblasts from the subventricular zone (SVZ, Hargus et al., 2008), which is a neurogenic center in the developing and adult brain, we compared the number of Dcx^+ neuroblasts residing in the SVZ and those detaching from the SVZ to migrate towards grafts consisting of either NSCs or iNSCs (Fig. 2E–H). In both groups, endogenous Dcx^+ neuroblasts appeared at similar numbers in the SVZ (Fig. 2E, H) and migrated to a similar extent towards the engrafted cells in the striatum (Fig. 2F–H).

We next compared whole genome, neural and metabolic gene expression profiles of transplanted NSCs and iNSCs (Fig. 2I–O). To this end, we isolated transplanted GFP^+ NSCs and iNSCs by fluorescence-activated cell sorting (FACS) from the rodent brains 14 days after engraftment (Fig. 2I). Transcriptome hierarchical cluster analyses indicated separation of engrafted NSCs and iNSCs from their *in vitro* counterparts, which is consistent with maturation of cells *in vivo* (Fig. 2J–L). Furthermore and similar to our observations *in vitro*, we observed minor, though detectable differences in the expression of aforementioned neural, oxidative and ER stress-associated genes, of heat shock protein-coding and of ubiquitination-associated genes in engrafted iNSCs and NSCs (Fig. 2M, Fig. S2A–D). We also determined DEGs in engrafted iNSCs in comparison to engrafted NSCs showing 428 upregulated and 356 downregulated genes (Fig. 2N). We found that upregulated genes in iNSCs were statistically enriched for GO terms such as *signal transduction*, *cellular homeostasis*, *cytokine activity*, *plasma membrane* or *extracellular space*, while downregulated genes in iNSCs were significantly enriched for terms such as *motor activity*, *cell membrane*, *organ development*, *cell cortex* and *cortex cytoskeleton* (see Table S2 for complete list of genes). We next determined the expression of regional identity genes in iNSCs and NSCs after transplantation into the adult forebrain (Fig. 2O). While NSCs retained their forebrain identity, transplanted iNSCs strongly expressed the caudal genes *Hoxd3*, *Hoxd4*, *Hoxa5* and *Hoxc6* and showed only mildly elevated levels of the forebrain-marker *Foxg1*. These findings indicated that caudal regional identities were vastly retained in transplanted iNSCs despite a prominent forebrain microenvironment surrounding engrafted cells.

4. Discussion

While iNSCs, NSCs and ESC–NPCs share global expression marks distinct from those in fibroblasts (Cassady et al., 2014), data is lacking on how cellular programs in these neural progenitor populations relate to each other. Our comparative transcriptome analysis revealed distinct global and neural profiles in iNSCs, which had higher similarities to those in brain-derived NSCs than to those in ESC–NPCs. Similar programs were also seen when comparing metabolic, stress- and cell cycle-associated marks in iNSCs, NSCs and ESC–NPCs. These findings could have significant implications for the use of iNSCs in biomedical research, as the close resemblance of self-renewing iNSCs and NSCs could be exploited for drug and toxicology screening assays or for disease modeling purposes. In fact, iNSCs may constitute a suitable, time- and cost-effective alternative cell source to pluripotent stem cell-derived neural cells when attempting characterization or modification of disease-related processes in brain-NSC-like cells and their progeny as, for instance, in neurodegenerative diseases. The potential of this approach is further heightened by the fact that iNSCs with neuronal and glial differentiation potential have recently been generated also from human fibroblasts using *SOX2* alone, though challenging, or using *SOX2* in combination with *HMGA2*/*anti-let7b* (Ring et al., 2012; Yu et al., 2015). Our data thus strongly encourage similar, thorough comparisons of neural cell identities in human NSCs, human iNSCs and in human pluripotent stem cell-derived NPCs, especially of patient-derived iNSCs and iPSC–NPCs and their derivatives, to identify optimal human stem cell populations for abovementioned screening and disease modeling purposes. By following a similar approach, we recently compared human iPSC–NPCs from different somatic origins and could demonstrate distinct origin-dependent neural programs in these cells (Hargus et al., 2014a).

An analysis of positional marks along the rostro-caudal axis revealed a hindbrain/posterior cell identity in iNSCs, which could be further shifted towards caudal and partially towards rostral but not towards ventral fates *in vitro*. Hence, our iNSCs may not be well suited to generate floor plate cells *in vitro* as similarly seen for our forebrain-derived NSCs that were cultured in parallel. On the other hand, iNSCs readily acquired caudal marks and might thus be applicable for repair of caudal neural domains such as the spinal cord. In line with this observation, transplanted iNSCs promoted functional recovery in a rodent model of spinal cord injury when generated by an identical protocol (Hong et al., 2014) or by a protocol using *Sox2* alone for direct neural conversion (Liu et al., 2015).

Similar to our *in vitro* results, transplanted iNSCs exhibited *in vivo*-characteristics, transcriptome profiles, neural and metabolic programs similar to those of transplanted NSCs. In contrast to engrafted forebrain NSCs, however, transplanted iNSCs strongly expressed caudal regional marker genes and only marginally acquired rostral gene expression. Thus, iNSCs vastly retained their caudal positional identity *in vivo* suggesting regional stability and a predominantly cell-autonomous regulation of positional marks in transplanted cells in a forebrain microenvironment. These findings are in line with observed limited plasticity of iNSCs in establishing rostral domains *in vitro* and indicated that rostral cell patterning of iNSCs most likely requires strong guidance cues and even employment of rostral transcription factors such as *Foxg1* (Lujan et al., 2012) or *Wnt7b* during earlier phases of iNSC generation before the establishment of a committed iNSC stage *in vitro*. It should be noted though that improper positional programs in transplanted iNSCs did not affect their integrity or the migration of endogenous neuroblasts from the SVZ. It remains to be shown how iNSCs with either rostral or caudal positional marks influence outcomes after transplantation into forebrain domains in animal models of neurological disease and injury. Furthermore, it would be important to determine the mechanisms, by which iNSCs acquire neural, positional programs during neural conversion. These studies would not only advance the field of direct reprogramming *in vitro* but could also provide important data for the emerging field of transcription factor-mediated neural reprogramming *in vivo*.

Supplementary data to this article can be found online at http://dx.doi.org/10.1016/j.scr.2016.04.015.

Accession numbers

The data discussed in this publication have been deposited in NCBI's Gene Expression Omnibus and are accessible through GEO Series accession number GSE73722 (http://www.ncbi.nlm.nih.gov/geo/query/acc.cgi?token=ydyrsqoyttaztqb&acc=GSE73722).

Author contributions

A-LH, HRS, TK, GH developed and designed the study and wrote the paper. A-LH, CZ, VS, ME, HZ, GH performed experiments. OEP, DWH, NT provided reagents. A-LH, CZ, MJA-B, VS, ME, HZ, GH analyzed data.

Acknowledgements

We would like to thank Ingrid Gelker, Martina Sinn, Martin Stehling, Elke Hoffmann and Claudia Kemming for outstanding technical assistance. This study was supported by research funding from the IMF at University Hospital Münster to GH (I-HA-111219) and from the DFG to TK (SFB-TRR128-B7). The authors declare no conflict of interest.

References

Bertacchi, M., Pandolfini, L., Murenu, E., Viegi, A., Capsoni, S., Cellerino, A., Messina, A., Casarosa, S., Cremisi, F., 2013. The positional identity of mouse ES cell-generated neurons is affected by BMP signaling. Cell. Mol. Life Sci. 70, 1095–1111.

Cassady, J.P., D'Alessio, A.C., Sarkar, S., Dani, V.S., Fan, Z.P., Ganz, K., Roessler, R., Sur, M., Young, R.A., Jaenisch, R., 2014. Direct lineage conversion of adult mouse liver cells and B lymphocytes to neural stem cells. Stem Cell Rep. 3, 948–956.

Ehrlich, M., Hallmann, A.L., Reinhardt, P., Arauzo-Bravo, M.J., Korr, S., Ropke, A., Psathaki, O.E., Ehling, P., Meuth, S.G., Oblak, A.L., et al., 2015. Distinct neurodegenerative changes in an induced pluripotent stem cell model of frontotemporal dementia linked to mutant TAU protein. Stem Cell Rep. 5, 83–96.

Han, D.W., Tapia, N., Hermann, A., Hemmer, K., Hoing, S., Arauzo-Bravo, M.J., Zaehres, H., Wu, G., Frank, S., Moritz, S., et al., 2012. Direct reprogramming of fibroblasts into neural stem cells by defined factors. Cell Stem Cell 10, 465–472.

Hargus, G., Cui, Y., Schmid, J.S., Xu, J., Glatzel, M., Schachner, M., Bernreuther, C., 2008. Tenascin-R promotes neuronal differentiation of embryonic stem cells and recruitment of host-derived neural precursor cells after excitotoxic lesion of the mouse striatum. Stem Cells 26, 1973–1984.

Hargus, G., Cooper, O., Deleidi, M., Levy, A., Lee, K., Marlow, E., Yow, A., Soldner, F., Hockemeyer, D., Hallett, P.J., et al., 2010. Differentiated Parkinson patient-derived induced pluripotent stem cells grow in the adult rodent brain and reduce motor asymmetry in Parkinsonian rats. Proc. Natl. Acad. Sci. U. S. A. 107, 15921–15926.

Hargus, G., Ehrlich, M., Arauzo-Bravo, M.J., Hemmer, K., Hallmann, A.L., Reinhardt, P., Kim, K.P., Adachi, K., Santourlidis, S., Ghanjati, F., et al., 2014a. Origin-dependent neural cell identities in differentiated human iPSCs in vitro and after transplantation into the mouse brain. Cell Rep. 8, 1697–1703.

Hargus, G., Ehrlich, M., Hallmann, A.L., Kuhlmann, T., 2014b. Human stem cell models of neurodegeneration: a novel approach to study mechanisms of disease development. Acta Neuropathol. 127, 151–173.

Hemmer, K., Zhang, M., van Wullen, T., Sakalem, M., Tapia, N., Baumuratov, A., Kaltschmidt, C., Kaltschmidt, B., Scholer, H.R., Zhang, W., et al., 2014. Induced neural stem cells achieve long-term survival and functional integration in the adult mouse brain. Stem Cell Rep. 3, 423–431.

Hong, J.Y., Lee, S.H., Lee, S.C., Kim, J.W., Kim, K.P., Kim, S.M., Tapia, N., Lim, K.T., Kim, J., Ahn, H.S., et al., 2014. Therapeutic potential of induced neural stem cells for spinal cord injury. J. Biol. Chem. 289, 32512–32525.

Kim, J., Efe, J.A., Zhu, S., Talantova, M., Yuan, X., Wang, S., Lipton, S.A., Zhang, K., Ding, S., 2011. Direct reprogramming of mouse fibroblasts to neural progenitors. Proc. Natl. Acad. Sci. U. S. A. 108, 7838–7843.

Kim, S.M., Flasskamp, H., Hermann, A., Arauzo-Bravo, M.J., Lee, S.C., Lee, S.H., Seo, E.H., Storch, A., Lee, H.T., Scholer, H.R., et al., 2014. Direct conversion of mouse fibroblasts into induced neural stem cells. Nat. Protoc. 9, 871–881.

Kriks, S., Shim, J.W., Piao, J., Ganat, Y.M., Wakeman, D.R., Xie, Z., Carrillo-Reid, L., Auyeung, G., Antonacci, C., Buch, A., et al., 2011. Dopamine neurons derived from human ES cells efficiently engraft in animal models of Parkinson's disease. Nature 480, 547–551.

Liu, C., Huang, Y., Pang, M., Yang, Y., Li, S., Liu, L., Shu, T., Zhou, W., Wang, X., Rong, L., et al., 2015. Tissue-engineered regeneration of completely transected spinal cord using induced neural stem cells and gelatin-electrospun poly (lactide-co-glycolide)/polyethylene glycol scaffolds. PLoS One 10, e0117709.

Lujan, E., Chanda, S., Ahlenius, H., Sudhof, T.C., Wernig, M., 2012. Direct conversion of mouse fibroblasts to self-renewing, tripotent neural precursor cells. Proc. Natl. Acad. Sci. U. S. A. 109, 2527–2532.

Reinhardt, P., Schmid, B., Burbulla, L.F., Schondorf, D.C., Wagner, L., Glatza, M., Hoing, S., Hargus, G., Heck, S.A., Dhingra, A., et al., 2013. Genetic correction of a LRRK2 mutation in human iPSCs links parkinsonian neurodegeneration to ERK-dependent changes in gene expression. Cell Stem Cell 12, 354–367.

Ring, K.L., Tong, L.M., Balestra, M.E., Javier, R., Andrews-Zwilling, Y., Li, G., Walker, D., Zhang, W.R., Kreitzer, A.C., Huang, Y., 2012. Direct reprogramming of mouse and human fibroblasts into multipotent neural stem cells with a single factor. Cell Stem Cell 11, 100–109.

Ross, C.A., Akimov, S.S., 2014. Human-induced pluripotent stem cells: potential for neurodegenerative diseases. Hum. Mol. Genet. 23, R17–R26.

Sheng, C., Zheng, Q., Wu, J., Xu, Z., Wang, L., Li, W., Zhang, H., Zhao, X.Y., Liu, L., Wang, Z., et al., 2012. Direct reprogramming of Sertoli cells into multipotent neural stem cells by defined factors. Cell Res. 22, 208–218.

Thier, M., Worsdorfer, P., Lakes, Y.B., Gorris, R., Herms, S., Opitz, T., Seiferling, D., Quandel, T., Hoffmann, P., Nothen, M.M., et al., 2012. Direct conversion of fibroblasts into stably expandable neural stem cells. Cell Stem Cell 10, 473–479.

Yu, K.R., Shin, J.H., Kim, J.J., Koog, M.G., Lee, J.Y., Choi, S.W., Kim, H.S., Seo, Y., Lee, S., Shin, T.H., et al., 2015. Rapid and efficient direct conversion of human adult somatic cells into neural stem cells by HMGA2/let-7b. Cell Rep.